Solar Energy 180 (2019) 351–359

Contents lists available at ScienceDirect

Solar Energy

journal homepage: www.elsevier.com/locate/solener

Solar light-driven complete mineralization of aqueous gram-positive and gram-negative bacteria with ZnO photocatalyst

Ahed Zyoud[a], Raed Alkowni[b], Omayma Yousef[c], Mazen Salman[d], Safaa Hamdan[d], Muath H. Helal[a], Sawsan F. Jaber[a], Hikmat S. Hilal[a,*]

[a] SSERL, Department of Chemistry, An-Najah National University, Nablus, Palestine
[b] Department of Biology & Biotechnology, An-Najah National University, Nablus, Palestine
[c] Department of Environmental Science, An-Najah National University, Nablus, Palestine
[d] Department of Horticultural and Agricultural Extension, Palestine Technical University-Kadoorie (PTUK), P.O. Box 7, Tulkarm, West Bank, Palestine

ARTICLE INFO

Keywords:
Solar
Complete mineralization
Gram-positive (Enterococcus faecium)
Gram-negative (Proteus mirabilis)
ZnO photocatalyst

ABSTRACT

ZnO nanoparticles have been effectively used in water disinfection from two common types of gram-positive (*Enterococcus faecium*) and gram–negative (*Proteus mirabilis*) bacteria under simulated solar radiations by inactivation. Complete mineralization of organic contents that leach out of inactivated bacteria has also been achieved leaving no soluble organic matter in water. Bacterial inactivation and complete mineralization have been confirmed by plate counting, high performance liquid chromatography and total organic content measurement. Effects of different reaction parameters (pH, temperature, bacterial concentration, reaction time and ZnO catalyst loading) have all been studied. Control experiments with Cut-off filters confirm the role of the UV tail in solar simulated light in the photocatalytic process. The results highlight the feasibility of using ZnO photocatalyst in complete disinfection of water from both hazardous *Enterococcus* and *Proteus mirabilis* bacteria, leaving no organic matters after degradation.

1. Introduction

Water pollution with hazardous chemicals and microorganisms is known (Gleick, 1993; Gleick and Palaniappan, 2010; Islam and Tanaka, 2004; Pandey et al., 2014; Vadde et al., 2018). Different water purification methods are known, such as peroxidation, ozonolysis chlorination and filtration. Despite their effectiveness, such methods have shortcomings (Yoo, 2018). Some are costly and non-accessible to needy societies. Filtration needs filter regeneration. Chlorination may yield hazardous chlorinated hydrocarbons (Benson et al., 2017). Low cost, safe and sustainable purifications, based on direct-solar light, are being heavily assessed (Hilal et al., 2007; Markowska-Szczupak et al., 2018; Zyoud et al., 2016; Zyoud et al., 2011; Zyoud et al., 2010). Photocatalysis using TiO_2, combined with H_2O_2 by UV irradiation, has been described for inactivation of different bacteria (Lanao et al., 2010) and (Lanao et al., 2012). Another report described using TiO_2 and UV-A irradiation in water disinfection by bacterial inactivation (Gumy et al., 2006).

Bacterial inactivation by ZnO nanoparticles is known. ZnO particles inactivate bacteria by rupturing their surfaces, in the dark (Sirelkhatim et al., 2015) and under UV irradiation (Markowska-Szczupak et al., 2018; Zyoud et al., 2017b). In literature (Keane et al., 2014; Loeb et al., 2017) attention is paid to bacterial inactivation, without describing what happens thereafter (Zyoud et al., 2016; Zyoud et al., 2017b).

After bacterial cell-wall rupturing, the organic contents leach into water. With heavy pollution, the resulting organic contaminants may exceed the limit of total organic content in water (0.05 mg/L) (Drinking water Quality Standards, 2003). Such issue is still not targeted (Dědková et al., 2014).

Recently we showed that ZnO nanoparticles photocatalyze complete mineralization of gram-negative bacteria (*E. coli*), and their organic content, using UV tail (~5%) of solar radiations (Zyoud et al., 2016; Zyoud et al., 2017b). Such recent studies are restricted to Gram-negative bacteria with thin cell walls only and cannot be generalized for other types.

This study involves two types of pathogenic bacteria, Gram-negative (represented by *Proteus mirabilis*) and Gram-positive (represented by *Enterococci faecium*). Both bacteria are hazardous and both are widely spread in natural waters (Devriese et al., 1993; Gonzalez and Infections, 2015; Hoge et al., 1991; Jacobsen and Shirtliff, 2011). A major difference between the two bacteria is the cell wall composition and thickness. Gram-positive bacteria have cell-walls with thicker peptidoglycan

* Corresponding author.
E-mail addresses: sawsan-jaber92@hotmail.com (S.F. Jaber), hshilal@najah.edu (H.S. Hilal).

https://doi.org/10.1016/j.solener.2019.01.034
Received 24 November 2018; Received in revised form 8 January 2019; Accepted 10 January 2019
0038-092X/ © 2019 Elsevier Ltd. All rights reserved.

layers. The major questions to answer here are: Is ZnO catalyzed photodegradation an effective method to disinfect water from both types of bacteria, despite their cell wall differences? Will ZnO completely photomineralize both types of bacteria leaving no organic matters in the treated water? Is solar simulated light effective in mineralization of the bacteria under natural working conditions? Is the photocatalytic process (using the UV tail in solar light) technically feasible for safe water disinfection from bacteria? These questions will be answered here for the first time.

The ZnO nanoparticles are intentionally chosen, as low-cost non-hazardous material. Zinc is described in human food supplements (Ninh et al., 1996) and plant fertilizers (Cakmak and Kutman, 2018). ZnO nanoparticles are semiconductors having band-gap ~3.2 eV (Lachheb et al., 2002; Sakthivel et al., 2003) with high absorptivity in the UV tail at ~387 nm. They are excited to produce OH· radicals, believed to be responsible for photodegrading aqueous organics (Gupta and Bahadur, 2018; Ong et al., 2018). The ability of ZnO nanoparticles to catalyze inactivation and complete mineralization of Gram-negative and Gram-positive bacteria, using simulated solar light under ambient conditions, is examined here. Effects of different parameters are also described.

2. Materials and methods

2.1. Chemicals

Common materials were all purchased from Frutarom Aldrich-Sigma (analytical grade). Clinically isolated Gram negative *Proteus mirabilis* was obtained from microbiological laboratories of ANU. Commercial Gram positive *Enterococcus faecium* (ATCC 700221) was used. Both bacteria were cultured on proper media onto Petri-dishes for use.

2.2. Equipment

A LaboMed, Inc. spectrophotometer was used for bacterial suspension quantifications. A Shimadzu-UV-1601 spectrophotometer was used for suspended ZnO nanoparticle spectral measurement. A Perkin-Elmer S55 photoluminescence spectrometer was used to measure photoluminescence (PL) spectra for aqueous ZnO nanoparticle suspensions. Scanning electronic micrographs (FE-SEM) were measured on Jeol-Model-JSM-6700F microscope at ICMCB (Bordeaux). X-ray diffraction (XRD) patterns were measured on a Philips XRD-XPERT-PRO diffractometer with a Cu-Ka source ($\lambda = 1.5418$ Å) at ICMCB (Bordeaux).

For high performance liquid chromatography (HPLC), a 1525-Binary-Waters equipment, with dual absorbance (2998 photodiode array detector at 250 nm), was used. A P/N7725i injection valve-filter (20 μL loop) was used for soluble species. A 6x250 mm HPLC-symmetry C18 column, 5 μm particles, was used. The mobile phase involved aqueous H_3PO_4 (1%) and methanol (30:70). Room temperature elution was performed at 1.0 mL/min flow rate. Peak area was calculated using a Breez integrator. A TELEDYNE-TEKMAR TOC FUSION equipment, carbon detection range 2 ppb–10,000 ppm, at PTUK, was used for total organic content (TOC) measurement. Each TOC value was measured three times, and the average value was calculated together with the standard deviation.

A tungsten-halogen solar simulator lamp was used in photodegradation experiments. Radiation intensity was measured and maintained at (100000 Lux, 0.0146 W/cm^2, 5% UV tail) using a lux-meter (Lx-102).

2.3. ZnO nanoparticle preparation

Preparation of ZnO nanoparticles was performed as described earlier (Zyoud et al., 2018; Zyoud et al., 2017a; Zyoud et al., 2017b). Aqueous $ZnCl_2$ solution (250 mL, 0.45 M) was used in preparation. NaOH (250 mL, 0.90 M) was placed inside a beaker and stirred at ~55 °C. The $ZnCl_2$ solution was added drop-wise (~40 min). The mixture was stirred for 2 h. Resulting white precipitate was taken, rinsed with deionized water, air-dried and annealed at 450 °C for 1 h.

2.4. Bacterial culturing and quantification

Stock solutions of $BaCl_2{\cdot}2H_2O$ (1.175% w/v, 0.096 N) and H_2SO_4 (1.00% v/v, 0.36 N) were prepared for the McFarland solution (0.50 M). Aliquots of H_2SO_4 (9.95 mL) and $BaCl_2$ (0.05 mL) solutions were mixed together. Solution optical density was spectrophotometrically measured (at λ_{max} 625 nm) to be in the range 0.08–0.10. This is equivalent to that for bacterial concentration 1.5x10^8 cfu/mL. The McFarland solution was a reference to spectrophotometrically quantify bacterial solutions of 1.5×10^8 cfu/mL. NaCl (normal saline 0.9%), NaOH (0.25 M) and HCl (0.25 M) solutions were used for disinfection experiment pH solution control.

Microorganism inoculum preparation was made using a nutrient broth. Nutrient broth media (28 g in 1.00 L) were prepared according to manufacturer (Oxoid Co.) instructions.

Plate counting was used to count bacteria in a given mixture. Bacterial solution (1.0 mL, 1.5×10^8 cfu/mL) corresponding to standard McFarland was micro-pipetted and diluted in a series of saline solutions (0.10 to 0.01 dilution factors). Aliquots (100 μL) of each diluted solution were cultured on two nutrient agar plates. The plates were incubated at 37 °C (± 1) for 24 h, and average numbers of bacterial colonies in two plates were counted. All counts were made in duplicates, and average count was taken. In case of inconsistent counts (more than 5% difference) additional confirmation counts were made. Counting was performed for bacterial measurement before and after photodegradation experiments.

The average bacterial concentration (cfu/mL) was calculated as shown in Eq. (1):

$$\text{Bact conc(cfu/mL)} = \text{number of counted colonies} \times \text{dil fact} \times 10 \quad (1)$$

where bact conc is bacterial concentration, dil fact is dilution factor.

Bacterial %loss was calculated as follows:

$$\frac{\text{Bacterial conc}_{in.} - \text{Bacterial conc}_{fin.}}{\text{Bacterial conc}_{in.}} \times 100\% \quad (2)$$

where *in* and *fin* refer to initial and final respectively.

2.5. Photocatalytic experiments

Bacterial disinfection experiments were conducted in 100 mL glass beakers, magnetically stirred and thermostated in a water bath. To each beaker was added 50 mL of water pre-contaminated with known volume of 5×10^5 cfu/mL bacteria with broth. In a typical photo-degradation experiment: ZnO (0.1 g) was suspended in pre-contaminated water (50 mL water with bacteria). The stirred mixture was irradiated from above for 30 min at 30 ± 3 °C. Dark experiments were performed using stirred ZnO (0.1 g) in pre-contaminated water (50 mL with bacteria) in the dark. Control photodegradation experiments were performed with no ZnO. Other control experiments were conducted in the dark with no ZnO. The measured bacterial solution, together with the broth inside, was used as value for initial bacterial counting and for initial TCO measurement. Each measurement was repeated three times, and the average value was calculated together with the standard deviation. Additional control experiments were conducted for broth solutions with no bacteria, using ZnO and light.

3. Results and discussion

3.1. ZnO characterization

The ZnO nano particle catalyst was prepared as described above

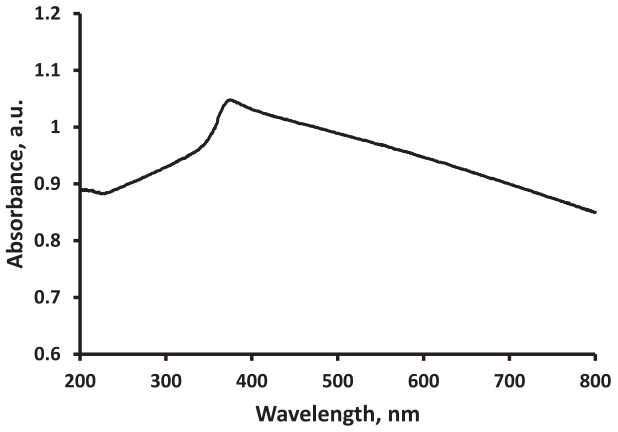

Fig. 1. Electronic absorption spectrum for ZnO nano-powder. Spectrum measured for aqueous suspension against water baseline.

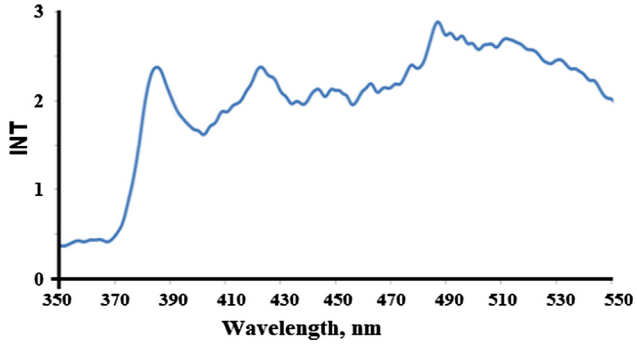

Fig. 2. Emission spectrum measured for ZnO nanopowder as aqueous suspension.

based on earlier reports. The powder was characterized only for confirmation. Solid electronic absorption spectrum, Fig. 1, for ZnO, measured for aqueous suspensions using water as base line, shows absorption peak at 373 nm, in congruence with earlier values (Zyoud et al., 2017b). PL spectrum for suspended ZnO, Fig. 2, using excitation wavelength 325 nm, shows a peak at 385 nm in congruence with literature (Raoufi, 2013; Talam and Karumuri, 2012; Zhao et al., 2016). Additional peaks observed at 423 nm and 487 nm are due to oxygen vacancies (Huang et al., 2001; Lopez-Romero, 2009) and surface defects (Zhao et al., 2016). Based on Tauc method and on PL emission peak at 385 nm, the band gap for the ZnO particles is ~3.23 eV. The results confirm that the prepared white solid is ZnO, as compared to earlier literature.

XRD pattern, measured for the solid powder here and in earlier work (Zyoud et al., 2017a), as shown in Fig. 3, further confirms the prepared ZnO. Characteristic reflections, (1 0 1), (1 0 0), (0 0 2), (1 0 2), (1 1 0), (1 0 3) and (1 1 2), (Akhtar et al., 2012; Arefi and Rezaei-Zarchi, 2012), for ZnO are all observed. Average particle size calculated using Scherrer's formula from the planes (1 0 0), (0 0 2), (1 0 1) and (1 0 2) was 27.2 nm. The XRD pattern thus confirms nano-size nature of the ZnO. The measured band gap ~3.2 eV here resembles literature (Lin et al., 2005; Mai et al., 2018).

The ZnO nano-size particles (27.2 nm based on XRD) exist inside larger (~200 nm) agglomerates, as observed by SEM, Fig. 4.

The characterization results confirm the nano-size nature of the prepared ZnO particles.

3.2. Enterococcus disinfection

Exposure of *Enterococcus* aqueous bacterial suspensions to solar simulated radiation, with ZnO nanoparticles, affects them. Under certain

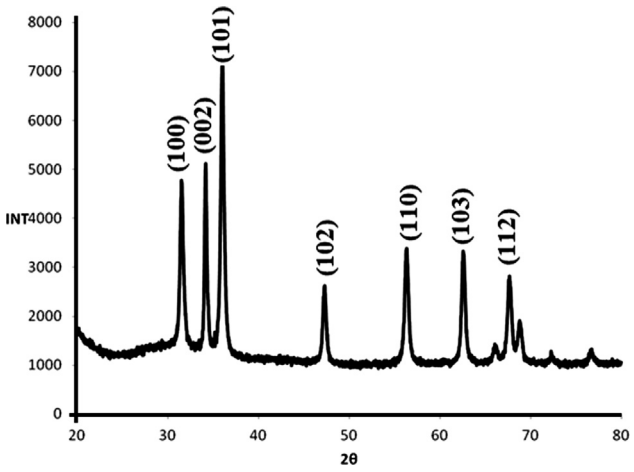

Fig. 3. XRD pattern measured for ZnO powder.

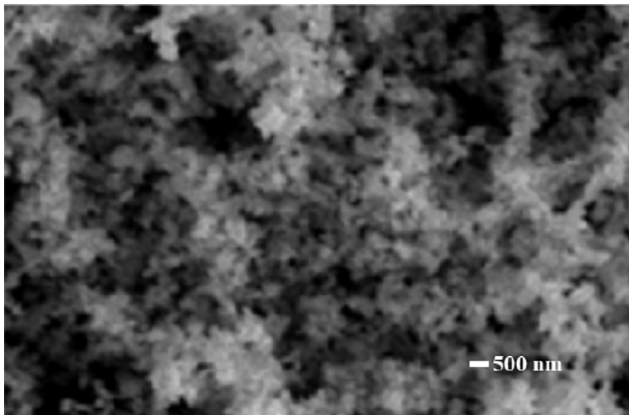

Fig. 4. SEM micrograph measured for ZnO powder.

conditions, complete bacterial loss is observed. The results are described below.

Control experiments were conducted in the absence of catalyst, light or both. Disinfection was conducted at 30 ± 3 °C and pH ~ 7.5 with initial bacterial concentration ~96000 cfu/mL. With no ZnO, only 23 ± 2% bacterial loss occurs after 30 min irradiation, due to UV tail, Table 1. With no ZnO, UV partly inactivates bacteria as described earlier (Blatchley et al., 2001). With ZnO (0.1 g) catalyst, in the dark, higher bacterial loss (51 ± 3%) occurs. This shows the ability of ZnO to affect the bacteria in the dark, as reported earlier (Sirelkhatim et al., 2015). When ZnO is used under light, complete bacterial loss is observed. Control experimental results thus confirm the role of ZnO in light-driven loss of aqueous *Enterococcus*. This shows the added value of irradiation on the bacterial inactivation, where ZnO is a photocatalyst, in congruence with literature (Keane et al., 2014). Effects of different parameters on percent loss of the bacteria are described.

Table 1
Enterococci %loss after 30 min under different photocatalytic conditions.

Experiment*	Remaining bacterial (cfu/mL)	Bacterial %loss
Dark/no Cat.	96,000 (± 5000)	00 (± 2)
Dark/Cat.	47,000 (± 3000)	51(± 3)
Light/no Cat	74,000 (± 3700)	23 (± 2)
Light/Cat.	300 (± 15)	99 (± 7)

* With broth added. Experiments conducted with ZnO (0.1 g) at ~30 °C and pH 7.5. (Initial bacterial concentration 96,000 (± 5000) cfu/mL in 50 mL).

Table 2
Effect of pH on *Enterococcus* bacterial %loss.

pH	Bacterial %loss with time			
	5 min	10 min	15 min	30 min
4.8	85 (± 4)	91(± 5)	93 (± 5)	99 (± 5)
7.5	81(± 4)	87 (± 4)	91(± 5)	99 (± 4)
9.6	77 (± 3)	83 (± 3)	88 (± 4)	99 (± 5)

Experiments conducted using Cat. (0.1 g) at ~29 °C for different times. (Bacterial concentration 96,000 (± 5000) cfu/mL inside 50 mL).

3.2.1. Effect of pH

Effect of pH on *Enterococcus* %loss has been studied. Three pH values (4.8, 7.5, and 9.6), spanning values for natural waters (Kulthanan et al., 2013) were intentionally examined. *Enterococci* live in a broad pH range 4.5–10 (Fisher and Phillips, 2009). Table 2 summarizes effect of pH on *Enterococci* %loss under irradiation with ZnO.

Table 2 shows that after 30 min, all bacteria are lost at all pH values. The pH effect is observed in shorter exposure times only (5, 10 or 15 min) where bacterial %loss is slightly lower at higher pH. This is due to electrostatic interactions with the catalyst surface. Despite being gram-positive, *Enterococci* have negatively charged surface membranes (Roy, 2009). With a zero-point charge 8.3–9.0 (Khataee et al., 2016; Raza et al., 2016) the ZnO surface becomes negatively charged at higher pH. The *Enterococci* are thus repelled away from the negatively charged surface. Similar behaviors are reported for ZnO interactions with other species (Akyol et al., 2004). However, if given enough time (30 min) complete bacterial loss is achieved. The results show the applicability of using the described process at different natural pH conditions.

3.2.2. Effect of temperature

Temperature effect on *Enterococci* %loss by photocatalysis has been studied. Three different temperatures (25, 30 and 35 °C) were chosen for practical purposes. Typically, natural waters have temperatures lower than 35 °C and *Enterococci* are especially active at 37 °C (Yang et al., 2018). Irradiation with ZnO catalyst is maintained for different times (5, 10 and 15 min). Table 3 summarizes the results. Within the temperature range used, temperature shows no significant effect on bacterial %loss. At all temperatures nearly complete bacterial loss is observed in 30 min. The 30 °C temperature is thus used hereinafter.

3.2.3. Effect of catalyst loading

Effect of ZnO photocatalyst loading, on *Enterococci* %loss has been studied, Table 4. The catalyst loadings used, 1.0–3.0 g/L, resemble those (1.5 and 3.1 mg mL^{-1}) described for other bacteria *S. aureus* and *E. coli* (Sirelkhatim et al., 2015; Xie et al., 2011). With higher catalyst loading, higher bacterial %loss occurs in short time (5 or 10 min). After longer time (30 min) nearly complete bacterial loss occurs for all loadings. Future pilot-plant scale study, with lower catalyst relative loadings, is thus recommended.

Effect of loading on catalyst relative efficiency, in terms of turnover frequency (TOF) and quantum yield (QY) is studied. Supplementary material S1 describes how the calculations are made. With higher catalyst loading, the efficiency (TOF) decreases, Table 4. This is known in photocatlytic reactions, due to screening of catalytic sites from radiation with higher loading (Hilal et al., 2010). The values of QY are not affected by catalyst loading because they are measured independent of catalyst loading (S1). The lowering in TOF and QY values with time is understandable, *vide infra*.

Table 3
Effect of temperature on *Enterococci* %loss.

Temp (°C)	Bacterial %Loss with time			
	5 min	10 min	15 min	30 min
25	51(± 3)	74 (± 4)	75 (± 5)	99 (± 4)
30	50 (± 4)	69 (± 4)	74 (± 4)	99 (± 5)
35	49 (± 3)	61 (± 3)	71 (± 4)	99 (± 6)

Experiments conducted using Cat. (0.1 g) and pH 7.5 for different times. Bacterial initial concentration 36,000 (± 2000) cfu/mL inside 50 mL).

3.2.4. Effect of bacterial concentration

The effect of *Enterococci* has been studied using three different concentrations (7800, 36,000 and 68000 cfu/mL) inside 50 mL mixtures. These high concentrations were intentionally chosen here, as they correspond to McFarland systems. Moreover, *Enterococci* may occur naturally at high concentrations. For example, *Enterococci* were observed in hospital sewage with concentrations of 10^4–10^6 cfu/100 mL (Anastasiou and Schmitt, 2011). Such values are normally lowered by mixing with municipality sewage to 10^4–10^5 cfu/100 mL. Table 5 shows bacterial %loss values observed for different *Enterococcus* concentrations. In 5 min, higher %loss occurs for higher bacterial concentration. After 10 min, the values become closer to one another. After 30 min, complete bacterial loss occurs for different concentrations. The results highlight the future prospects of using the photocatalytic system described here for water disinfection. Complete bacterial loss, after 30 min, indicates the process feasibility to inactivate bacteria at lower concentrations that may remain after short times.

To study effect of *Enterococci* concentration on ZnO photocatalyst relative efficiency, TOF and QY were calculated, while keeping other parameters unchanged. Values for TOF and QY increase readily with increased bacterial concentration, Table 5. With higher concentration, more bacteria are exposed to oxidizing species resulting from light irradiation. Entries 1 & 2 show that increasing bacterial concentration by ~7 fold increases catalyst TOF and QY by ~7.7. Similarly Entries 2 & 3 show that increasing bacterial concentration by ~2 increases TOF and QY by ~2. The results suggest first-order reaction with respect to bacterial concentration.

The Table shows that for same bacterial concentration, values of TOF and QY decrease with time. This is due to bacterial concentration lowering with time. This further confirms the effect of bacterial concentration on catalyst efficiency discussed above.

3.2.5. Enterococci complete mineralization

The results confirm the ability of the photocatalytic process to inactivate the *Enterococci*. Inactivation involves bacterial killing by cell wall rupturing (Baptista et al., 2018; Sarwar et al., 2016), *vide* Section 3.4. When the cell wall is ruptured, bacterial organic matters leach out to aqueous solution. This increases the aqueous organic matters, and adds to the organic content of the originally present broth soluble compounds. Therefore, bacterial inactivation itself increases aqueous soluble organics. In case of complete mineralization of the inactivated bacteria (and organic materials) the organic matter concentration in water is lowered.

Such assumptions are examined using HPLC analysis, with a filter-tipped syringe to eliminate insoluble materials. The HPLC peak area thus shows aqueous soluble organics only, Table 6.

Table 6, (entries 1–3) shows that soluble broth is photomineralized with enough time. Entry (4) shows that with no ZnO in the dark and zero bacterial loss within zero time, the soluble organic content has relatively low peak area. With ZnO in the dark, after 30 min, 51 ± 3% bacterial loss occurs and the organic peak area is still relatively low, Entry (5). This means that not much of the organic matter leaches from the inactivated bacteria. Similarly Entry (6) shows low organic content in water as only 23 ± 2% bacterial inactivation occurs.

Entry (7) shows that after 30 min under photocatalytic reaction conditions, with complete bacterial loss, more aqueous organics leach out to aqueous phase. The photodegradation process thus completely inactivates the bacteria and pushes out their organic matter, with little

Table 4
Effect of ZnO loading on its photocatalytic efficiency in *Enterococci* inactivation.

Mass Cat. (g)	5 min			10 min			15 min			30 min		
	%Loss	TOF	QY	%Loss	TOF	QY	%Loss	TOF	QY	%Loss	TOF	QY
0.05	64 (± 3)	12.5×10^{-18}	10.4×10^{-15}	70 (± 4)	6.8×10^{-18}	5.7×10^{-15}	87 (± 5)	5.6×10^{-18}	4.8×10^{-15}	99 (± 5)	3.2×10^{-18}	2.7×10^{-15}
0.10	71 (± 4)	6.9×10^{-18}	11.6×10^{-15}	73 (± 4)	3.6×10^{-18}	6.0×10^{-15}	89 (± 5)	2.9×10^{-18}	4.9×10^{-15}	99 (± 6)	1.6×10^{-18}	2.7×10^{-15}
0.15	83 (± 5)	5.4×10^{-18}	13.7×10^{-15}	87 (± 5)	2.8×10^{-18}	7.1×10^{-15}	94 (± 6)	2.0×10^{-18}	5.2×10^{-15}	99 (± 6)	1.1×10^{-18}	2.7×10^{-15}

Experiments conducted at 30 °C and pH 7.5 for different times. (Bacterial concentration 36,000 (± 2000) cfu/mL in 50 mL).

Table 5
Effect of *Enterococci* initial concentration on ZnO catalyst efficiency.

Entry No.	Init. Conc. cfu/mL	5 min			10 min			30 min		
		%Loss	TOF	QY	%Loss	TOF	QY	%Loss	TOF	QY
1	7800 (± 400)	40 (± 2)	0.84×10^{-18}	0.5×10^{-15}	68 (± 3)	0.72×10^{-18}	0.45×10^{-15}	99 (± 5)	0.14×10^{-18}	0.22×10^{-15}
2	36,000 (± 2000)	67 (± 4)	6.5×10^{-18}	4.1×10^{-15}	72 (± 4)	3.5×10^{-18}	2.2×10^{-15}	99 (± 4)	1.6×10^{-18}	1.03×10^{-15}
3	68,000 (± 3500)	64 (± 3)	1.2×10^{-18}	7.5×10^{-15}	71 (± 3)	6.5×10^{-18}	4.2×10^{-15}	99 (± 4)	3.03×10^{-18}	1.94×10^{-15}

Experiments conducted with different initial concentrations of bacteria in 50 mL, using Cat. (0.1 g) at 30 °C and pH 7.5 for different irradiation times.

mineralization. Entry (8) shows that in longer photodegradation time (240 min), the bacteria and their organic content, together with remains of soluble broth, are completely mineralized.

Complete *Enterococci* inactivation and mineralization is thus achievable by photocatalysis under solar simulated light.

TOC results further confirm complete mineralization, Table 7. TOC values show all organic content existing in the gross reaction mixture, including insoluble organics.

Entries (1–2) show that when broth is treated alone under photocatalytic experimental conditions for 30 min, it mineralizes almost completely (99 ± 1%). Entries (3–5) show that the TOC value in the gross reaction mixture is nearly unchanged without photocatalysis. Overall organic content in reaction mixture remains constant before and after bacterial inactivation.

Entry (6) shows that the TOC value is lowered in photocatalytic reaction mixture after 30 min irradiation. All bacteria are inactivated, as described above, in 30 min irradiation. However, TOC value is still relatively high reaching ~60% of original organic matter. Thus only part of inactivated bacterial organics is completely mineralized, as the measured TOC is due to non-mineralized organic matter and others.

Entry (7) shows that after enough irradiation time (240 min), the TOC value becomes lower with only 18 ppm left. More mineralization of leaching organic matters occurs. The 18 ppm value is attributed to remains of solid bacterial cell wall fragments. *Enterococci* are gram-positive bacteria with relatively thick walls (Hancock et al., 2014). The wall involves a peptidoglycan backbone and anionic polymers which comprise ~90% of the cell wall mass (Hancock et al., 2014) whereas proteins comprise only 10% of cell wall mass. The peptidoglycan backbone is well known (Kolenbrander and Ensign, 1968) for its rigid framework, which resists photomineralization here. Ability of bacterial walls to resist photomineralization was reported (Zyoud et al., 2017b).

Table 7
TOC values for *Enterococci* photocatalytic disinfection.

Entry No.	Conditions	TOC value (ppm)
1	Broth/Dark/no Cat.	15 (± 2)
2	Broth/Light/ZnO Cat (30 min)	0.11(± 0.03)
3	Bacteria/Dark/No Cat.* (30 min)	45 (± 5)
4	Bacteria/Light/ No Cat.* (30 min)	42 (± 4)
5	Bacteria/Dark/Cat.* (30 min)	44 (± 4)
6	Bacteria/Light/Cat* (30 min)	29 (± 3)
7	Bacteria/Light/Cat* (240 min)	18 (± 2)

* With broth added. Experiments conducted in 50 mL mixture at 30 °C and pH 7.5. Cat. loading (0.1 g). (Bacterial concentration 96,000 (± 5000) cfu/mL in 50 mL).

3.3. *Proteus mirabilis* disinfection

Proteus mirabilis is a gram-negative bacterial series. Gram-negative bacteria, including *Proteus mirabilis*, have plasma membranes and cell walls including outer membranes, peptidoglycan layers and periplasms. Compared to *Enterococcus*, *Proteus mirabilis* have thinner cell wall, with much thinner peptidoglycan back bone (Beveridge, 1999). Photodegradation of hazardous *Proteus Mirabilis* is assessed here.

Control experiments have been conducted as shown in Table 8. In the dark, ZnO causes Gram-negative bacterial inactivation as described earlier. With no ZnO, irradiation shows no significant effect on the bacteria. In the dark, 31 ± 2% loss is observed by the ZnO powder within 30 min. Compared to *Enterococci* (Table 1), sensitivity to ZnO is lower for the *Proteus mirabilis* in the dark. The results are in congruence with earlier studies, where Gram-negative bacteria (*E. coli*) are more resistive than gram-positive bacteria (*S. aureus*) to ZnO (Emami-Karvani and Chehrazi, 2011; Jain et al., 2013). Under irradiation with ZnO

Table 6
Loss percentage and HPLC peak area of *Enterococci* disinfection.

Entry Number	Experiment	Reaction time	Bacterial %loss	Peak area (μV. sec.)
1	Cat./Broth only/Light	00	= =	80,000 (± 4000)
2	Cat./Broth only/light	30 min	= =	0 (± 400)
4	Bacteria/No Cat./dark*	0 min	0.00 (± 2)	90,199 (± 4500)
5	Bacteria/Cat./dark*	30 min	51.04 (± 3)	74,021 (± 3700)
6	Bacteria/Light/no Cat.*	30 min	22.92 (± 2)	67,686 (± 3400)
7	Bacteria/Cat./light*	30 min	99.7 (± 5)	220,528 (± 10000)
8	Bacteria/Cat./light*	240 min	100 (± 5)	0.00 (± 600)

* With broth added. Experiments conducted at 30 °C pH 7.5. Cat. loading (0.1 g). (Bacterial concentration 96,000 (± 5000) cfu/mL in 50 mL).

Table 8
Values of *Proteus mirabilis* %loss under different conditions.

Experiment	Remaining bacterial concentration (cfu/mL)	%Loss (± 5%)
No Cat./Dark	94,000 (± 5000)	0 (± 1)
Cat./dark	65,000 (± 3500)	31 (± 2)
Light/no Cat.	86,000 (± 4300)	9 (± 1.5)
Cat./light	200 (± 10)	100 (± 7)

Experiments conducted at 30 °C and pH 7.5 in 30 min. (*Proteus mirabilis* initial concentration 94,000 (± 5000) cfu/mL inside 50 mL).

Table 9
Effect of pH on *Proteus mirabilis* %loss.

pH	Bacterial %loss with time			
	5 min	10 min	15 min	30 min
4.3	92 (± 5)	94 (± 5)	97 (± 5)	99 (± 5)
7.4	86 (± 4)	95 (± 5)	97 (± 5)	99 (± 4)
8.9	77 (± 3)	82 (± 4)	83(± 4)	99 (± 5)

Experiments conducted using Cat. (0.1 g) at 30 °C for different times (bacterial concentration 94,000 (± 5000) cfu/mL in 50 mL).

complete bacterial loss is achieved after 30 min. Photodegradation (subject matter here) is thus feasible to inactivate Gram-negative bacteria, as the case with Gram-positive bacteria. Effects of different reaction parameters on the photodegradation process are discussed below.

3.3.1. Effect of pH

Effect of pH (4.3, 7.4, and 8.9) on *Proteus mirabilis* photocatalytic inactivation has been studied over different time periods (5, 10 and 15 min), Table 9. For acidic and neutral conditions there is no significant difference in bacterial %loss, as observed for short times. At higher pH (8.9) the %loss values are lowered. Negative cell wall charges in *Proteus mirabilis* cell membrane (Czerwonka et al., 2016) make them slightly retarded away from ZnO negative surface at higher pH, as discussed for *Enterococci*. In 30 min, complete *Proteus mirabilis* loss occurs by photocatalysis at all pH values.

3.3.2. Effect of temperature

Effect of temperature on *Proteus mirabilis* has been studied. The bacteria have high growth at temperatures ranging 23–25 °C (Thompson, 2018). This study involves different temperatures 25, 30 and 35 °C, Table 10. Temperature does not affect photocatalytic process for different exposure times. At all temperatures, complete loss of *Proteus mirabilis* is observed. In this respect, *Proteus mirabilis* bacteria resemble *Enterococci* discussed above, while the former bacteria are more sensitive to photodegradation in shorter irradiation times.

With no significant difference between different temperatures, the temperature of choice to study other parameters below is 30 °C. This is intentionally made for better comparison with *Enterococci* described above.

Table 10
Effect of temperature on *Proteus mirabilis* bacterial %loss.

Temp (°C)	Bacterial %loss with time			
	5 min	10 min	15 min	30 min
25	93 (± 5)	96 (± 5)	98(± 5)	99 (± 5)
29	93 (± 4)	95 (± 4)	98 (± 5)	99 (± 5)
35	93 (± 5)	97 (± 5)	98(± 4)	99 (± 5)

Experiments conducted using Cat. (0.1 g) and pH 7.5 for different times (Bacterial concentration 69,000 (± 3500) cfu/mL in 50 mL).

3.3.3. Effect of catalyst loading

Effect of ZnO catalyst loading, on *Proteus mirabilis* inactivation, has been studied, Table 11. With increased catalyst loading, bacterial %loss slightly increases, since more catalytic sites are available and used in the reaction. After enough exposure time, complete bacterial loss is achieved with different loadings. This shows the possibility of using small catalyst loading to achieve complete disinfection, as described above for *Enterococci*. Literature shows similar findings where increased catalyst ($Ag@TiO_2$) loading increased the photocatalysis rate in bacterial disinfection (Sreeja and Shetty, 2017).

TOF for ZnO, in *Proteus mirabilis* inactivation, has been studied, Table 11. With increased catalyst loading, the TOF decreases in all reaction times. Again, there is a need for pilot plant testing with lower catalyst loading. Despite that, complete bacterial inactivation is still achievable in 30 min. Effect of catalyst loading on QY is not observed, as QY values are calculated independent of catalyst amount.

3.3.4. Effect of bacterial concentration

Effect of *Proteus mirabilis* bacterial initial concentration, on the photocatalytic inactivation, has been studied, Table 12. In short times, bacterial %loss increases with higher initial concentration. After 30 min 99% loss occurs in all cases.

As initial concentration increases the relative catalyst efficiency increases. Entries 1–2 show that by ~5 fold bacterial concentration increase, TOF and QY values increase by ~5 fold. When increasing concentration by ~1.4 fold, TOF and QY values increase by ~1.4 fold (Entries 2–3). Similar to *Enterococci*, the results again suggest a first-order reaction with respect to the bacterial concentration under the working conditions, particularly for short time (5 and 10 min) measurements. Complete inactivation of *Proteus mirabilis* shows the feasibility of using phtocatalysis in future disinfection processes.

3.3.5. Proteus mirabilis complete mineralization

Complete photomineralization of inactivated *Proteus mirabilis* bacteria by ZnO is assessed. HPLC analysis of the aqueous phase, of the reaction-mixture, is performed as described for *Enterococci* above, Table 13, while excluding solid materials. Broth complete mineralization is described in Section 3.2.5. Like *Enterococci*, soluble organic concentration increase indicates bacterial inactivation by cell wall rupturing.

Entry (1) confirms presence of soluble organics in water, due to soluble broth and others. Entry (2) shows higher soluble organics than Entry (1), which confirms bacterial inactivation and organic leaching. Entry (3) shows partial inactivation of bacteria by photocatalysis.
Entry (4) shows remarkable increase in soluble organics in water. Compared with Entry (2), this indicates higher photocatalytic process efficiency to inactivate the bacteria within 30 min, with more organic material leaching.
Entry (5) shows no organics left in aqueous phase after 240 min. Like *Enterococci*, the inactivated *Proteus mirabilis* bacteria are completely mineralized together with their soluble organic content and soluble broth.

Measured TOC values confirm HPLC results, Table 14. TOC results involve all soluble and insoluble organics of reaction mixture.

Entries (1–2) show broth photomineralization, as discussed for *Enterococci*. Entries (3–5) show that TOC values remain unchanged after reaction cessation. This resembles above findings where ZnO inactivates *Proteus mirabilis* without photomineralizing them. Entry (6) shows lower TOC after 30 min, which means that some organics are mineralized. After 240 min, all organic matter is photomineralized (Entry 7). The 2.5 ppm value is attributed to solid material remains such as cell wall fragments. The value is lower than for *Enterococci* (Entry 7, Table 7) as the *Proteus mirabilis* bacteria are Gram-negative, with much

Table 11
Effect of catalyst loading on its photocatalytic efficiency in *Proteus mirabilis* bacterial disinfection.

Mass Cat. (g)	5 min			10 min			15 min			30 min		
	%Loss	TOF	QY	%Loss	TOF	QY	%Loss	TOF	QY	%Loss	TOF	QY
0.05	68 (± 3)	35×10^{-18}	11×10^{-15}	84 (± 4)	21.3×10^{-18}	6.8×10^{-15}	90 (± 4)	15.2×10^{-18}	4.8×10^{-15}	99 (± 5)	8.4×10^{-18}	2.7×10^{-15}
0.10	76 (± 4)	19.3×10^{-18}	12.2×10^{-15}	85 (± 4)	11×10^{-18}	6.8×10^{-15}	93 (± 5)	7.9×10^{-18}	5.0×10^{-15}	99 (± 5)	4.2×10^{-18}	2.7×10^{-15}
0.15	75 (± 4)	12.7×10^{-18}	12.1×10^{-15}	87 (± 5)	7.4×10^{-18}	7.0×10^{-15}	93 (± 5)	5.3×10^{-18}	5.0×10^{-15}	99 (± 5)	2.8×10^{-18}	2.7×10^{-15}

Experiments conducted at 30 °C and pH 7.5 for different irradiation times (bacterial initial concentration 94,000 (± 5000) cfu/mL in 50 mL).

Table 12
Effect of *Proteus mirabilis* initial concentration on their inactivation.

Entry No.	Init. cfu/mL	5 min			10 min			30 min		
		%Loss	TOF	QY	%Loss	TOF	QY	%Loss	TOF	QY
1	15,000 (± 750)	75 (± 3)	3.04×10^{-18}	1.9×10^{-15}	82 (± 4)	1.7×10^{-18}	1.1×10^{-15}	99 (± 5)	0.67×10^{-18}	0.48×10^{-15}
2	96,000 (± 5000)	86 (± 4)	22.3×10^{-18}	14.2×10^{-15}	95 (± 5)	12.3×10^{-18}	7.8×10^{-15}	99 (± 5)	4.28×10^{-18}	2.76×10^{-15}
3	130,000 (± 65000)	89 (± 4)	31.3×10^{-18}	19.8×10^{-15}	96 (± 5)	16.9×10^{-18}	7.9×10^{-15}	99 (± 5)	5.8×10^{-17}	3.73×10^{-15}

Experiments conducted using Cat. (0.1 g) at 30 °C and pH 7.5 for different times.

Table 13
HPLC results for soluble organics from *Proteus mirabilis* photomineralization.

Entry no.	Experiment	Reaction time	Percentage of loss	Peak area (μV. sec.)
1	No Cat./dark	0 min	0.00 (± 2)	33,765 (± 1700)
2	Cat./dark	30 min	30.85 (± 2)	42,690 (± 2100)
3	Light/no cat.	30 min	8.51 (± 0.5)	60,794 (± 3000)
4	Cat./light	30 min	99.79 (± 5)	140,402 (± 6500)
5	Cat./light	240 min	100 (± 5)	0.00 (± 650)

Experiments conducted at 30 °C and pH 7.5 with Cat. (0.1 g) using 94,000 (± 5000) cfu/mL in 50 mL.

Table 14
TOC values for reaction mixture remaining after photodegradation of *Proteus mirabilis*.

Entry No.	Experiment	TOC value (ppm)
1	Broth/Dark/no Cat.	15 (± 2)
2	Broth/Light/ZnO Cat (30 min)	0.11 (± 0.02)
3	Bacteria/Dark/No Cat.*	60 (± 6)
4	Bacteria/Light/ No Cat.*	55 (± 5)
5	Bacteria/Dark/Cat.*	58 (± 6)
6	Bacteria/Light/Cat* (30 min)	22 (± 3)
7	Bacteria/Light/Cat* (240 min)	2.5 (± 0.3)

* With broth added. Experiments conducted at 30 °C pH 7.5 and bacteria (94000 (± 5000) cfu/mL, 50 mL). Cat. loading (0.1 g).

thinner insoluble peptidoglycan layer than *Enterococci* (Gram-positive).

3.4. Mode of action of ZnO nanoparticles

The ability of ZnO nanoparticles to inactivate different bacteria is known, but the mechanism is debatable, especially in the dark. Many reports suggest that ZnO nanoparticles themselves cause cell wall rupturing for bacterial inactivation (Adams et al., 2006; Brayner et al., 2006; Li et al., 2011; Sirelkhatim et al., 2015; Zhang et al., 2007). Others suggest that the Zn^{2+} ions, coming out from ZnO particles, are responsible for inactivation (Li et al., 2011; Sirelkhatim et al., 2015; Song et al., 2010), which is challenged by others (Sarwar et al., 2016). Reports suggest that the Zn^{2+} ions are nutrients rather than inhibitors for bacteria (Espitia et al., 2012). Kaolinite-supported ZnO were confirmed to have photocatalytic inactivation of different bacteria (Dědková et al., 2015). ZnO nanoparticle role to inactivate bacteria in the dark is beyond the scope of this work. The subject matter here is photocatalytic bacterial inactivation followed by complete mineralization.

Inactivation, of both bacteria, is more pronounced under radiation than in the dark. This indicates photocatalysis by the ZnO themselves. ZnO particles are semiconductors with band-gap ~3.2 eV. Therefore, radiations of 388 nm wavelengths or shorter may excite ZnO nanoparticles. This is confirmed by control experiments performed on different bacteria (Zyoud et al., 2016; Zyoud et al., 2017b). Cut-off filters are used to block radiations with 400 nm and shorter wavelength photons from photocatalytic mixtures. There is no effect for light, and bacterial %loss resembles that observed for ZnO system in the dark. Therefore, ZnO nanoparticle photocatalytic behavior is limited to UV. Solar simulated light spectrum involves ~5% as a UV tail, which is the active radiation responsible for bacterial inactivating. Similar results are known for light/H_2O_2 driven *enterococci* inactivation using TiO_2, where UV is strictly needed (Lanao et al., 2012).

Moreover, experiments with cu-off filters show no mineralization for different bacteria or their organic content (Zyoud et al., 2016; Zyoud et al., 2017b). This means that the UV tail is again responsible for mineralization of bacterial organic matters.

Under UV, the photocatalytic bacterial disinfection is a multi-step process:

1) Excitation of ZnO particles with UV tail photons. A photon (with enough energy) creates an electron-hole pair. The electron, in the conduction band, may reduce nearby aqueous species, while the hole oxidizes others at the other end. These processes are well described for TiO_2 and ZnO nano particles in aqueous systems. Different active species are produced such as H_2O_2, O_2^- in addition to the OH· radical. Details of such species are described earlier (Alam et al., 2018; Lee et al., 2016; Yi et al., 2018) and need not be described again. The radical is believed to oxidize different organics in water.
2) Bacterial cell-wall rupturing by the excited ZnO nano particle itself and/or other resulting active species in water. Bacterial organic contents leach out into water (Baptista et al., 2018; Sarwar et al., 2016) and become exposed to active species.
3) Complete oxidation of the leaching out aqueous organic species if given enough time. Such organic compounds are completely mineralized in water just like other well-known organic compounds reported earlier (Bhatia and Verma, 2017; Mohamed and Abu-Dief, 2018; Munshi et al., 2018). Chloramphenicol has been degraded in water by the photo-phenton process using Fe^{2+} ions and H_2O_2 under

light (Trovó et al., 2013).

Remaining stable solid species, such as peptidoglycan fragments, resist photodegradation. Such species account for the TOC values remaining in reaction mixture after photocatalytic reaction cessation as described above, where the Gram-positive bacteria with thicker walls yield higher remaining TOC than Gram-positive bacteria.

With promising prospects of complete photomineralization, the results show the necessity for more study on photocatalytic processes to disinfect water, focusing on complete mineralization of the resulting organic contents. For better understanding, work is underway here to assess photocatalytic process effectiveness on other Gram-positive and Gram-negative bacteria. Photocatalyst recovery and reuse after reaction cessation is considered by supporting ZnO on insoluble surfaces. Kaolinite-supported ZnO particles inactivate different types of bacteria through photocatalysis, which makes them worth to further study in future complete photomineralization (Dědková et al., 2015). Stan-alone study of the kinetics of the photocatalytic process is also targeted here. Pilot-plant scale study on naturally polluted waters is worth to do.

4. Conclusion

ZnO nanoparticles partly inactivate *Enterococcus faecium* (Gram-positive) and *Proteus mirabilis* (Gram-negative) bacteria in dark. Under solar simulated UV radiation complete bacterial inactivation occurs in 30 min. In 240 min, complete bacterial and organic matter photomineralization is achieved. Cell-wall fragments resist photomineralization. ZnO photocatalyst functions under different experimental conditions, making it useful for natural-water disinfection.

Acknowledgment

Based on O.Y. thesis, financed by ANU-Palestine, under A.Z. and R.A. co-supervision. Additional experiments are made (A.Z. & R.A). Guy Campet (ICMCB-Bordeuax) helped in XRD & SEM measurements. M.Z. and S.H. measured TOC. M.H.H. added literature and ideas. H.S.H. formulated problem, design & writing.

Conflict of interest

This work carries no conflicts of interests.

Appendix A. Supplementary material

Supplementary data to this article can be found online at https://doi.org/10.1016/j.solener.2019.01.034.

References:

Adams, L.K., Lyon, D.Y., Alvarez, P.J., 2006. Comparative eco-toxicity of nanoscale TiO_2, SiO_2, and ZnO water suspensions. Water Res. 40 (19), 3527–3532.
Akhtar, M.J., Ahamed, M., Kumar, S., Khan, M.M., Ahmad, J., Alrokayan, S.A., 2012. Zinc oxide nanoparticles selectively induce apoptosis in human cancer cells through reactive oxygen species. Int. J. Nanomed. 7, 845.
Akyol, A., Yatmaz, H., Bayramoglu, M., 2004. Photocatalytic decolorization of remazol red RR in aqueous ZnO suspensions. Appl. Catal. B 54 (1), 19–24.
Alam, U., Khan, A., Ali, D., Bahnemann, D., Muneer, M., 2018. Comparative photocatalytic activity of sol–gel derived rare earth metal (La, Nd, Sm and Dy)-doped ZnO photocatalysts for degradation of dyes. RSC Adv. 8 (31), 17582–17594.
Anastasiou, I., Schmitt, H., 2011. Hospital-associated Enterococcus faecium in the water chain. RIWA-Rhine, Nieuwegein.
Arefi, M.R., Rezaei-Zarchi, S., 2012. Synthesis of zinc oxide nanoparticles and their effect on the compressive strength and setting time of self-compacted concrete paste as cementitious composites. Int. J. Mol. Sci. 13 (4), 4340–4350.
Baptista, P.V., McCusker, M.P., Carvalho, A., Ferreira, D.A., Mohan, N.M., Martins, M., Fernandes, A.R., 2018. Nano-strategies to fight multidrug resistant bacteria—"A Battle of the Titans". Front. Microbiol. 9, 1441.
Benson, N.U., Akintokun, O.A., Adedapo, A.E., 2017. Disinfection byproducts in drinking water and evaluation of potential health risks of long-term exposure in Nigeria. J. Environ. Public Health 2017, 7535797. https://doi.org/10.1155/2017/7535797.
Beveridge, T.J., 1999. Structures of gram-negative cell walls and their derived membrane vesicles. J. Bacteriol. 181 (16), 4725–4733.
Bhatia, S., Verma, N., 2017. Photocatalytic activity of ZnO nanoparticles with optimization of defects. Mater. Res. Bull. 95, 468–476.
Blatchley, E., Dumoutier, N., Halaby, T., Levi, Y., Laine, J., 2001. Bacterial responses to ultraviolet irradiation. Water Sci. Technol. 43 (10), 179–186.
Brayner, R., Ferrari-Iliou, R., Brivois, N., Djediat, S., Benedetti, M.F., Fiévet, F., 2006. Toxicological impact studies based on Escherichia coli bacteria in ultrafine ZnO nanoparticles colloidal medium. Nano Lett. 6 (4), 866–870.
Cakmak, I., Kutman, U., 2018. Agronomic biofortification of cereals with zinc: a review. Eur. J. Soil Sci. 69 (1), 172–180.
Czerwonka, G., Guzy, A., Kałuża, K., Grosicka, M., Dańczuk, M., Lechowicz, Ł., Gmiter, D., Kowalczyk, P., Kaca, W., 2016. The role of proteus mirabilis cell wall features in biofilm formation. Arch. Microbiol. 198 (9), 877–884.
Dědková, K., Janíková, B., Matějová, K., Peikertová, P., Neuwirthová, L., Holešinský, J., Kukutschová, J., 2015. Preparation, characterization and antibacterial properties of ZnO/kaoline nanocomposites. J. Photochem. Photobiol., B 148, 113–117.
Dědková, K., Matějová, K., Lang, J., Peikertová, P., Kutláková, K.M., Neuwirthová, L., Frydrýšek, K., Kukutschová, J., 2014. Antibacterial activity of kaolinite/nanoTiO_2 composites in relation to irradiation time. J. Photochem. Photobiol., B 135, 17–22.
Devriese, L., Pot, B., Collins, M., 1993. Phenotypic identification of the genus Enterococcus and differentiation of phylogenetically distinct enterococcal species and species groups. J. Appl. Bacteriol. 75 (5), 399–408.
Emami-Karvani, Z., Chehrazi, P., 2011. Antibacterial activity of ZnO nanoparticle on gram-positive and gram-negative bacteria. African J. Microbiol. Res. 5 (12), 1368–1373.
Espitia, P.J.P., Soares, N.d.F.F., dos Reis Coimbra, J.S., de Andrade, N.J., Cruz, R.S., Medeiros, E.A.A., 2012. Zinc oxide nanoparticles: synthesis, antimicrobial activity and food packaging applications. Food Bioprocess Technol. 5 (5), 1447–1464.
Fisher, K., Phillips, C., 2009. The ecology, epidemiology and virulence of Enterococcus. Microbiology 155 (6), 1749–1757.
Gleick, P.H. (Ed.), 1993. Water in Crisis: A Guide to the Worlds Fresh Water Resources. Oxford University Press, Oxford.
Gleick, P.H., Palaniappan, M., 2010. Peak water limits to freshwater withdrawal and use. Proc. Natl. Acad. Sci. 107 (25), 11155–11162.
Gonzalez, G., Proteus Infections, in: Drugs and Diseases, ed. Bronze, M., Medscape; 2015.
Gumy, D., Rincon, A.G., Hajdu, R., Pulgarin, C., 2006. Solar photocatalysis for detoxification and disinfection of water: different types of suspended and fixed TiO_2 catalysts study. Sol. Energy 80 (10), 1376–1381.
Gupta, J., Bahadur, D., 2018. Defect-mediated reactive oxygen species generation in Mg-substituted ZnO nanoparticles: efficient nanomaterials for bacterial inhibition and cancer therapy. ACS Omega 3 (3), 2956–2965.
Hancock, L.E., Murray, B.E., Sillanpää, J. Enterococcal cell wall components and structures; 2014.
Hilal, H., Majjad, L., Zaatar, N., El-Hamouz, A., 2007. Dye-effect in TiO_2 catalyzed contaminant photo-degradation: sensitization vs. charge-transfer formalism. Solid State Sci. 9 (1), 9–15.
Hilal, H.S., Al-Nour, G.Y., Zyoud, A., Helal, M.H., Saadeddin, I., 2010. Pristine and supported ZnO-based catalysts for phenazopyridine degradation with direct solar light. Solid State Sci. 12 (4), 578–586.
Hoge, C.W., Adams, J., Buchanan, B., Sears, S.D., 1991. Enterococcal bacteremia: to treat or not to treat, a reappraisal. Rev. Infect. Dis. 13 (4), 600–605.
Huang, M.H., Wu, Y., Feick, H., Tran, N., Weber, E., Yang, P., 2001. Catalytic growth of zinc oxide nanowires by vapor transport. Adv. Mater. 13 (2), 113–116.
Drinking water Quality Standards. 2003. Edstrom Industries, Waterford, Wisconsin. Webpage: https://docplayer.net/23457533-Drinking-water-quality-standards.html.
Islam, M.S., Tanaka, M., 2004. Impacts of pollution on coastal and marine ecosystems including coastal and marine fisheries and approach for management: a review and synthesis. Mar. Pollut. Bull. 48 (7–8), 624–649.
Jacobsen, S.M., Shirtliff, M.E., 2011. Proteus mirabilis biofilms and catheter-associated urinary tract infections. Virulence 2 (5), 460–465.
Jain, A., Bhargava, R., Poddar, P., 2013. Probing interaction of Gram-positive and Gram-negative bacterial cells with ZnO nanorods. Mater. Sci. Eng., C 33 (3), 1247–1253.
Keane, D.A., McGuigan, K.G., Ibáñez, P.F., Polo-López, M.I., Byrne, J.A., Dunlop, P.S., O'Shea, K., Dionysiou, D.D., Pillai, S.C., 2014. Solar photocatalysis for water disinfection: materials and reactor design. Catal. Sci. Technol. 4 (5), 1211–1226.
Khataee, A., Kiranşan, M., Karaca, S., Arefi-Oskoui, S., 2016. Preparation and characterization of ZnO/MMT nanocomposite for photocatalytic ozonation of a disperse dye. Turk. J. Chem. 40 (4), 546–564.
Kolenbrander, P., Ensign, J., 1968. Isolation and chemical structure of the peptidoglycan of Spirillum serpens cell walls. J. Bacteriol. 95 (1), 201–210.
Kulthanan, K., Nuchkull, P., Varothai, S., 2013. The pH of water from various sources: an overview for recommendation for patients with atopic dermatitis. Asia Pacific Allergy 3 (3), 155–160.
Lachheb, H., Puzenat, E., Houas, A., Ksibi, M., Elaloui, E., Guillard, C., Herrmann, J.-M., 2002. Photocatalytic degradation of various types of dyes (alizarin S, crocein orange G, methyl red, congo red, methylene blue) in water by UV-irradiated titania. Appl. Catal. B 39 (1), 75–90.
Lanao, M., Ormad, M., Goñi, P., Miguel, N., Mosteo, R., Ovelleiro, J., 2010. Inactivation of clostridium perfringens spores and vegetative cells by photolysis and TiO_2 photocatalysis with H_2O_2. Sol. Energy 84 (4), 703–709.
Lanao, M., Ormad, M., Mosteo, R., Ovelleiro, J., 2012. Inactivation of Enterococcus sp. by photolysis and TiO_2 photocatalysis with H_2O_2 in natural water. Sol. Energy 86 (1), 619–625.
Lee, K.M., Lai, C.W., Ngai, K.S., Juan, J.C., 2016. Recent developments of zinc oxide based photocatalyst in water treatment technology: a review. Water Res. 88, 428–448.
Li, M., Zhu, L., Lin, D., 2011. Toxicity of ZnO nanoparticles to Escherichia coli:

mechanism and the influence of medium components. Environ. Sci. Technol. 45 (5), 1977–1983.
Lin, K.-F., Cheng, H.-M., Hsu, H.-C., Lin, L.-J., Hsieh, W.-F., 2005. Band gap variation of size-controlled ZnO quantum dots synthesized by sol–gel method. Chem. Phys. Lett. 409 (4–6), 208–211.
Loeb, S., Li, C., Kim, J.-H., 2017. Solar photothermal disinfection using broadband-light absorbing gold nanoparticles and carbon black. Environ. Sci. Technol. 52 (1), 205–213.
Lopez-Romero, S., 2009. Growth and characterization of ZnO cross-like structures by hydrothermal method. Matéria (Rio de Janeiro) 14 (3), 977–982.
Mai, V.-T., Hoang, Q.-B., Mai, X.-D., 2018. Enhanced red emission in ultrasound-assisted sol-gel derived ZnO/PMMA nanocomposite. Adv. Mater. Sci. Eng. 2018, 7252809. https://doi.org/10.1155/2018/7252809.
Markowska-Szczupak, A., Rokicka, P., Wang, K., Endo, M., Morawski, A., Kowalska, E., 2018. Photocatalytic water disinfection under solar irradiation by d-glucose-modified titania. Catalysts 8 (8), 316.
Mohamed, W., Abu-Dief, A.M., 2018. Synthesis, characterization and photocatalysis enhancement of Eu_2O_3-ZnO mixed oxide nanoparticles. J. Phys. Chem. Solids 116, 375–385.
Munshi, G.H., Ibrahim, A.M., Al-Harbi, L.M., 2018. Inspired preparation of zinc oxide nanocatalyst and the photocatalytic activity in the treatment of methyl orange dye and paraquat herbicide. Int. J. Photoenergy 2018, 5094741. https://doi.org/10.1155/2018/5094741.
Ninh, N.X., Thissen, J.-P., Collette, L., Gerard, G., Khoi, H.H., Ketelslegers, J.-M., 1996. Zinc supplementation increases growth and circulating insulin-like growth factor I (IGF-I) in growth-retarded Vietnamese children. Am. J. Clin. Nutrit. 63 (4), 514–519.
Ong, C.B., Ng, L.Y., Mohammad, A.W., 2018. A review of ZnO nanoparticles as solar photocatalysts: synthesis, mechanisms and applications. Renew. Sustain. Energy Rev. 81, 536–551.
Pandey, P.K., Kass, P.H., Soupir, M.L., Biswas, S., Singh, V.P., 2014. Contamination of water resources by pathogenic bacteria. AMB Exp. 4 (1), 51.
Raoufi, D., 2013. Synthesis and photoluminescence characterization of ZnO nanoparticles. J. Lumin. 134, 213–219.
Raza, W., Faisal, S.M., Owais, M., Bahnemann, D., Muneer, M., 2016. Facile fabrication of highly efficient modified ZnO photocatalyst with enhanced photocatalytic, antibacterial and anticancer activity. RSC Adv. 6 (82), 78335–78350.
Roy, H., 2009. Tuning the properties of the bacterial membrane with aminoacylated phosphatidylglycerol. IUBMB Life 61 (10), 940–953.
Sakthivel, S., Neppolian, B., Shankar, M., Arabindoo, B., Palanichamy, M., Murugesan, V., 2003. Solar photocatalytic degradation of azo dye: comparison of photocatalytic efficiency of ZnO and TiO_2. Sol. Energy Mater. Sol. Cells 77 (1), 65–82.
Sarwar, S., Chakraborti, S., Bera, S., Sheikh, I.A., Hoque, K.M., Chakrabarti, P., 2016. The antimicrobial activity of ZnO nanoparticles against vibrio cholerae: variation in response depends on biotype. Nanomed. Nanotechnol. Biol. Med. 12 (6), 1499–1509.
Sirelkhatim, A., Mahmud, S., Seeni, A., Kaus, N.H.M., Ann, L.C., Bakhori, S.K.M., Hasan, H., Mohamad, D., 2015. Review on zinc oxide nanoparticles: antibacterial activity and toxicity mechanism. Nano-Micro Lett. 7 (3), 219–242.
Song, W., Zhang, J., Guo, J., Zhang, J., Ding, F., Li, L., Sun, Z., 2010. Role of the dissolved zinc ion and reactive oxygen species in cytotoxicity of ZnO nanoparticles. Toxicol. Lett. 199 (3), 389–397.
Sreeja, S., Shetty, V., 2017. Photocatalytic water disinfection under solar irradiation by Ag@ TiO_2 core-shell structured nanoparticles. Sol. Energy 157, 236–243.
Talam, S., Karumuri, S.R., Gunnam, N., 2012. Synthesis, characterization, and spectroscopic properties of ZnO nanoparticles. ISRN Nanotechnology 2012.
Thompson, R., 2018. The isolation and characterisation of Proteus mirabilis bacteriophages and their effect on the colonisation and blockage of urinary catheters. University of the West of England.
Trovó, A.G., de Paiva, V.A., Machado, A.E., de Oliveira, C.A., Santos, R.O., 2013. Degradation of the antibiotic chloramphenicol by photo-Fenton process at lab-scale and solar pilot plant: kinetic, toxicity and inactivation assessment. Sol. Energy 97, 596–604.
Vadde, K.K., Wang, J., Cao, L., Yuan, T., McCarthy, A.J., Sekar, R., 2018. Assessment of water quality and identification of pollution risk locations in Tiaoxi river (Taihu watershed) China. Water 10 (2), 183.
Xie, Y., He, Y., Irwin, P.L., Jin, T., Shi, X., 2011. Antibacterial activity and mechanism of action of zinc oxide nanoparticles against Campylobacter jejuni. Appl. Environ. Microbiol. 77 (7), 2325–2331.
Yang, E., Fan, L., Yan, J., Jiang, Y., Doucette, C., Fillmore, S., Walker, B., 2018. Influence of culture media, pH and temperature on growth and bacteriocin production of bacteriocinogenic lactic acid bacteria. AMB Exp. 8 (1), 10.
Yi, Z., Wang, J., Jiang, T., Tang, Q., Cheng, Y., 2018. Photocatalytic degradation of sulfamethazine in aqueous solution using ZnO with different morphologies. R. Soc. Open Sci. 5 (4), 171457.
Yoo, J.-H., 2018. Review of disinfection and sterilization-back to the basics. Infect. Chemotherapy 50 (2), 101–109.
Zhang, L., Jiang, Y., Ding, Y., Povey, M., York, D., 2007. Investigation into the antibacterial behaviour of suspensions of ZnO nanoparticles (ZnO nanofluids). J. Nanopart. Res. 9 (3), 479–489.
Zhao, J.-H., Liu, C.-J., Lv, Z.-H., 2016. Photoluminescence of ZnO nanoparticles and nanorods. Optik-Int. J. Light Electron Opt. 127 (3), 1421–1423.
Zyoud, A., Ateeq, M., Helal, M.H., Zyoud, S.H., Hilal, H.S., 2018. Photocatalytic degradation of phenazopyridine contaminant in soil with direct solar light. Environ. Technol. 1–12.
Zyoud, A., Dwikat, M., Al-Shakhshir, S., Ateeq, S., Shteiwi, J., Zu'bi, A., Helal, M.H., Campet, G., Park, D., Kwon, H., 2016. Natural dye-sensitized ZnO nanoparticles as photo-catalysts in complete degradation of E. coli bacteria and their organic content. J. Photochem. Photobiol., A 328, 207–216.
Zyoud, A., Jondi, W., AlDaqqah, N., Asaad, S., Qamhieh, N., Hajamohideen, A., Helal, M.H., Kwon, H., Hilal, H.S., 2017a. Self-sensitization of tetracycline degradation with simulated solar light catalyzed by ZnO@ montmorillonite. Solid State Sci. 74, 131–143.
Zyoud, A., Zaatar, N., Saadeddin, I., Helal, M.H., Campet, G., Hakim, M., Park, D., Hilal, H.S., 2011. Alternative natural dyes in water purification: anthocyanin as TiO_2-sensitizer in methyl orange photo-degradation. Solid State Sci. 13 (6), 1268–1275.
Zyoud, A.H., Dwikat, M., Al-Shakhshir, S., Ateeq, S., Ishtaiwa, J., Helal, M.H., Kharoof, M., Alami, S., Kelani, H., Campet, G., 2017b. ZnO nanoparticles in complete photomineralization of aqueous gram negative bacteria and their organic content with direct solar light. Sol. Energy Mater. Sol. Cells 168, 30–37.
Zyoud, A.H., Zaatar, N., Saadeddin, I., Ali, C., Park, D., Campet, G., Hilal, H.S., 2010. CdS-sensitized TiO_2 in phenazopyridine photo-degradation: catalyst efficiency, stability and feasibility assessment. J. Hazard. Mater. 173 (1–3), 318–325.